PHYSICAL REVIEW B **93**, 081408(R) (2016)

Direct visualization of surface phase of oxygen molecules physisorbed on Ag(111) surface: A two-dimensional quantum spin system

Shunji Yamamoto,[1,*] Yasuo Yoshida,[1,†] Hiroshi Imada,[2] Yousoo Kim,[2] and Yukio Hasegawa[1]

[1]*The Institute for Solid State Physics, The University of Tokyo, 5-1-5, Kashiwa-no-ha, Kashiwa, Chiba 277-8581, Japan*

[2]*SISL RIKEN, 2-1 Hirosawa, Wako, Saitama 351-0198, Japan*

(Received 25 September 2015; revised manuscript received 28 January 2016; published 16 February 2016)

We report on the real-space observation of the two-dimensional distorted triangular lattice of physisorbed oxygen (O_2) molecules on an Ag(111) surface by low-temperature scanning tunneling microscopy. The physisorbed state of the O_2 monolayers was confirmed by measuring their thermal stability, which showed good agreement with previous thermal desorption spectroscopy. The distortion of the observed lattice was reproduced quantitatively by considering the intermolecular exchange interaction in Monte Carlo calculations, indicating a critical role of antiferromagnetic ordering of O_2 spins. In tunneling spectra, the Kondo resonance was not observed on the O_2 layer at 4.7 K unlike the case of physisorbed O_2 on Ag(110). These results indicate that an intrinsic $S = 1$ spin of the O_2 molecules was preserved to form a two-dimensional antiferromagnetic quantum spin system on the surface.

DOI: 10.1103/PhysRevB.93.081408

An oxygen molecule (O_2) has 16 electrons in its molecular orbitals to give the $^3\Sigma_g^-$ electronic configuration, i.e., the degenerated outermost orbitals (π^*_{2p}) have a half-filled configuration in the ground state [1]. Consequently, O_2 is one of the smallest molecular magnets with an $S = 1$ quantum spin, and its solid phase is known to be an antiferromagnetic Mott insulator [1,2]. This makes O_2 attractive as a unique source of new physics; it is a building block of the low-dimensional quantum spin systems, especially quantum spin liquid phases in two-dimensional (2D) frustrated lattices [3] and the Haldane phase with the one-dimensional (1D) arrangement [4]. Since the mid-1980s, research groups have extensively studied adsorbed O_2 molecules on the surfaces of highly ordered pyrolytic graphite (HOPG) [5] and hexagonal boron nitride [6] and inside 1D structures such as nanoporus coordination polymers [7,8] and single-walled carbon nanotubes [9] in order to observe such elusive phenomena. However, the available experimental techniques for investigating the physical properties of this molecule have been limited to spatial averaging ones. On the other hand, the development of scanning tunneling microscopy (STM) and spectroscopy (STS) has enabled direct access to the properties of single atoms and molecules and even their manipulation to fabricate artificial nanostructures. Combined with surface preparation methods under ultrahigh vacuum (UHV) conditions, STM can provide an ideal playground for bottom-up fabrication of low-dimensional spin systems in an atomically clean environment [10].

A well-known problem for O_2 adsorption on a substrate is that O_2 often loses its spin because of strong interactions with the substrate such as the charge transfer, formation of chemical bonds, and dissociative adsorption. However, a low-temperature low-energy electron diffraction (LEED) study recently revealed that the interaction between the physisorbed O_2 and Ag(111) surface is substantially weak and that structures almost identical to solid oxygen phases can be realized on the surface [11]. In addition, the existence of a spin in physisorbed O_2 on an Ag(111) substrate was confirmed by an experiment on the ortho-para conversion of molecular hydrogen [12]. Therefore, there is a strong need for STM-based techniques with single-molecule resolution in order to directly realize understanding of the structural and electronic properties and verify the potential of the O_2/Ag(111) system for low-dimensional quantum spin systems.

In this Rapid Communication, we report the direct visualization of O_2 physisorbed on Ag(111) by using low-temperature STM/STS. Physisorption of the observed monolayer O_2 islands was confirmed by a comparison with previous results from thermal desorption spectroscopy (TDS) [11]. In the islands, a well-ordered O_2 structure was observed, and the lattice was distorted from an isosceles triangular shape. The distortion can be explained by the competition between the magnetic and elastic instabilities of the O_2 lattice, and it was confirmed by a quantitative estimation of the distortion based on Monte Carlo (MC) calculations. We found no feature of the Kondo resonance in the differential tunneling conductance (dI/dV) spectra. Based on these observations and calculations, we discuss the realization of an $S = 1$ 2D antiferromagnetic quantum spin system.

All measurements were performed with a UHV ($<1 \times 10^{-8}$ Pa) low-temperature STM (Omicron LT-STM) at 4.7 K in RIKEN. The STM tips were electrochemically etched from high-purity (99.99%) Ag wires. A single-crystal Ag(111) sample was cleaned by repeated cycles of 1 keV Ar-ion sputtering and 700 K annealing. With the Ag(111) surface atom density defined as one monolayer (ML), about 0.3 ML of O_2 was deposited onto the Ag(111) surface held inside the STM. The surface temperature was raised to 12.6 K during the O_2 adsorption.

Figure 1(a) shows an STM image of O_2 on Ag(111) taken at 4.7 K. A number of depressed areas with the same depth ($\sim$0.05 nm) were observed. Because these areas did not exist prior to the O_2 deposition, we identified them as O_2 monolayer islands (see Supplemental Material for details [13]). The depressed contrast of the O_2 islands in the STM images is due to the reduced local density of states on the O_2-covered area from the Fermi level to the measured energy. A similar feature

*shunji-yamamoto@issp.u-tokyo.ac.jp

†Corresponding author: yyoshida@issp.u-tokyo.ac.jp

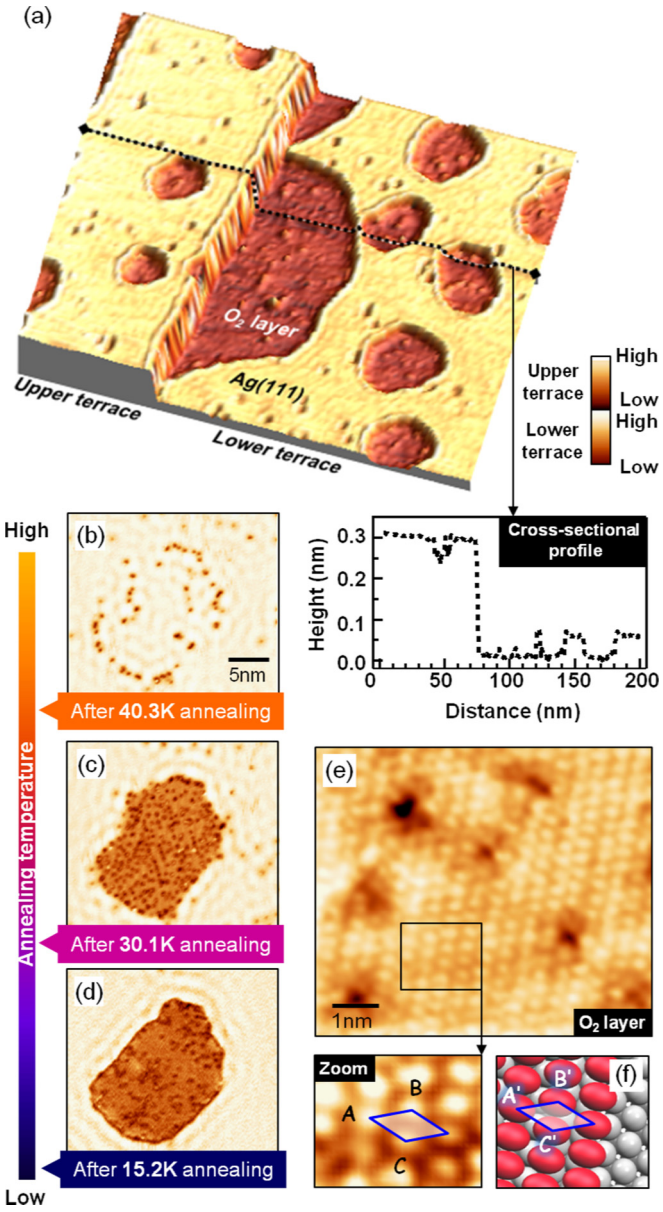

FIG. 1. (a) STM image acquired on O_2/Ag(111) at 4.7 K with a bare Ag tip and cross-sectional profile taken along the black dotted line. (b)–(d) STM images after annealing at (b) 40.3 K, (c) 30.1 K, and (d) 15.2 K. (e) Molecular resolution STM image of an O_2 island with an O_2 terminated tip and a zoomed image of the structure. (f) Schematic O_2 structure for the LC phase (red ellipsoids) on the Ag(111) surface (gray spheres) derived from LEED measurement [11] [(a) sample bias voltage: $V_s = -50$ mV, tunneling current: $I_t = 3$ pA; (b), (c) $V_s = 30$ mV, $I_t = 3$ pA; (d), (e) $V_s = 30$ mV, $I_t = 2$ pA].

has been reported for carbon monoxide monolayer islands physisorbed on Ag(111) [14]. The O_2 islands were easily displaced or desorbed by the tunneling current, which indicates a fairly low adsorption energy due to the physisorbed nature of the island (see Supplemental Material for details [13]). For this reason, all measurements in this work were carried out at a significantly low tunneling current ($|I_t| \leqslant 3$ pA) and sample bias voltage ($|V_s| \leqslant 200$ mV).

In order to confirm that the islands were physisorbed on the surface, we investigated the thermal stability of the O_2 islands by heating the sample in a stepwise fashion up to 40.3 K. Figures 1(b)–1(d) display STM images taken at 4.7 K after annealing at each temperature increment for 1 min. The number of defects in the O_2 islands gradually increased with annealing up to 30.1 K [Figs. 1(c) and 1(d)]. After the sample was annealed up to 40.3 K, most of the O_2 islands disappeared. These observations are in good agreement with the result of the TDS measurement, which showed a desorption peak at 35 K for the low-coverage (LC) phase of physisorbed O_2 on Ag(111) [11]. Therefore, we conclude that the observed islands were the physisorbed O_2 layer.

Figure 1(e) is a molecular resolution image of the O_2 layer showing a well-ordered lattice structure. The dimensions of the surface unit cell of the O_2 structure were measured to be $AB = 0.421 \pm 0.013$ nm, $AC = 0.435 \pm 0.013$ nm, and $\angle BAC = 42.8 \pm 1.1^\circ$ [blue parallelogram in the zoomed image of Fig. 1(e)] based on real-space STM images of three different O_2 islands. Note that it was a scalene triangular lattice (i.e., $AB < AC$), which is revealed more clearly in the reciprocal space. Figures 2(a)–2(c) display a 2D Fourier transform (FT) pattern of STM images showing an atomic resolution Ag(111) surface and the molecular resolution O_2 islands, respectively. The direction of the reciprocal vector of the Ag(111) surface is drawn as black dotted lines. There are six distinct peaks in Fig. 2(b), and the red arrows indicate vectors (P,Q,R) corresponding to the periodic structures of the O_2 rows in the islands. While R is along the reciprocal vector of the Ag(111) surface, P and Q are tilted from the black dotted lines by $11.5 \pm 0.5^\circ$ and $7.5 \pm 0.5^\circ$, respectively. The angular difference corresponds to the scalene triangular lattice of the O_2 molecules (i.e., $AB < AC$). The other pattern displayed in Fig. 2(c) was taken on a domain whose lattice is mirror inverted and thus should be equivalent to that of Fig. 2(b) because of the mirror symmetry of the Ag(111) substrate. The existence of the mirror-inverted domains indicates that the scalene triangular lattice is intrinsic to the present system.

The previous LEED study reported that two phases of O_2/Ag(111) exist depending on O_2 coverage [11] and that the O_2 orientations of the LC and high-coverage (HC) phases are parallel and perpendicular, respectively, to the Ag(111) substrate. Because the observed unit cell was close to that of the LC phase observed in the LEED study [$A'B' = A'C' = 0.43$ nm, $\angle B'A'C' = 43.7^\circ$, shown in Fig. 1(f)], we presumed that the phase in our system was LC. However, the LEED pattern showed that the O_2 layer forms an isosceles triangular lattice (i.e., $A'B' = A'C'$) instead of the scalene triangular one. In fact, the LEED spots which correspond to P and Q in the FT pattern of Fig. 2(b) are elongated; that is presumably due to the spatial averaging of the above-mentioned two equivalent domains. Therefore, we concluded that LEED and STM basically observed the same structure, but only STM could resolve the detailed structure of the LC phase by focusing on a single domain at a high spatial resolution.

The O_2 lattice was incommensurate with the Ag(111) substrate, which means that the surface corrugation of the substrate affects the O_2 lattice only as random perturbations leading the FT (or LEED) spots broad. Hence, the effect of the substrate can be ignored when discussing the shape of

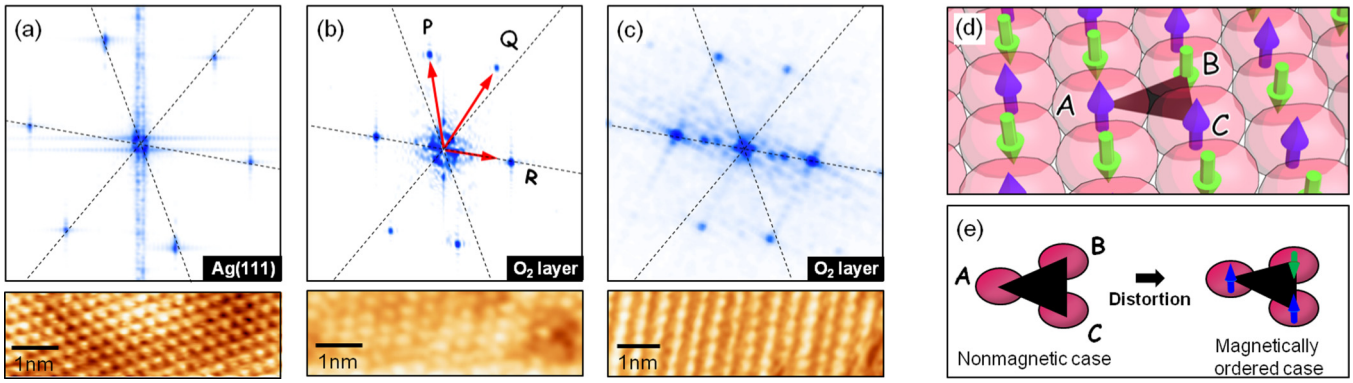

FIG. 2. Two-dimensional Fourier transform patterns of (a) the Ag(111) surface and (b), (c) O_2 islands, in which *P, Q,* and *R* indicate the reciprocal vector of the O_2 lattice. Corresponding STM images are also shown below. (b) and (c) are taken from mirror-inverted domains that are equivalent because of the mirror symmetry of the Ag(111) substrate. (d) Schematic O_2 lattice (red ellipsoids) for the LC phase on Ag(111). The blue and green arrows denote the directions of the O_2 spins. (e) Lattice distortion induced by antiferromagnetic ordering.

the O_2 lattice. Actually, an almost identical scalene triangular lattice was reported for LC phase of O_2 physisorbed on HOPG by LEED, and that is also incommensurate to the substrate [15]. This similarity of the O_2 structures on two different substrates indicates that the lattice structures are intrinsic to the O_2 molecules. Theoretically, however, when only van der Waals (vdW) and electric quadrupole–quadrupole (EQQ) interactions are considered, an isosceles triangular lattice (i.e., $AB = AC$) is stable for the LC phase of O_2 on HOPG [16], and an almost identical isosceles triangular lattice is favorable also for a 2D freestanding O_2 lattice from our MC calculations [13]. This suggests that there should be some reason for the lattice to be distorted (i.e., $AB < AC$) for physisorbed O_2 layers.

To explain the lattice structure, there may be exchange interactions between the O_2 spins. The energy of the exchange interactions between the O_2 spins was estimated by magnetization measurements of solid oxygen ($\lesssim$6 meV [1]). This was less than the electric interactions ($\lesssim$30 meV [1]) but still large enough to contribute to the total energy of the system. Namely, the exchange interactions can be a significant portion of the formation energy for the O_2 lattice [17]. Indeed, the HC phase of O_2/HOPG [18,19] and solid oxygen [1] showed lattice distortions coinciding with antiferromagnetic ordering, which indicates that the softness of the O_2 lattice allows the magnetic interaction to be strongly involved in the lattice formation. Although a magnetic order has not yet been observed in the LC O_2 phases, the preferred orientation of the O_2 spins was predicted by MC calculations in which magnetic interactions were simply added to the electric interactions [Fig. 2(d)] [19]. If the magnetic ordering is considered, the system can further reduce the energy by shortening the sides of the isosceles triangle at which spins are antiferromagnetically aligned, as shown in Fig. 2(e). This mechanism reasonably explains the lattice distortion (i.e., $AB < AC$) of the present system, while the previous calculation [19] does not predict such a magnetoelastic response in the LC phase.

To confirm the scenario, we performed MC calculations of the 2D freestanding O_2 lattice (see Supplemental Material for details [13]). Total Hamiltonian of the lattice is written by $\mathcal{H} = \mathcal{H}_{vdW} + \mathcal{H}_{EQQ} + \mathcal{H}_{Ex}$. Here, $\mathcal{H}_{vdW}$ and $\mathcal{H}_{EQQ}$ are a vdW interaction and an EQQ interaction respectively, and $\mathcal{H}_{Ex} = \sum_{i<j}^{N} J\, \boldsymbol{S}_i \cdot \boldsymbol{S}_j$ is an exchange interaction, where i and j denote the numbering of the O_2 molecules. In general, the exchange coupling J depends not only on the intermolecular distance but also on the molecular orientation [1,20]. This is because the exchange interaction originates from the overlap between the O_2 orbitals, which can be described by tight binding representation $J \sim 4t^2/U$ (Hubbard Hamiltonian) [20], where t is a transfer matrix element between the O_2 orbitals, and U is an on-site Coulomb potential. Taking into account this effect, we can simplify J as an exponential function [13]:

$$J \simeq J(\min_s[r_{s(ij)}]) = 2J_0 e^{-\gamma(\min_s[r_{s(ij)}]-R_0)}. \qquad (1)$$

Here $\min_s[r_{s(ij)}]$ is a function to take the minimum value in a set of the nonbonding-atom distances $r_{s(ij)}$ $(s = 1,2,3,4)$ shown in Fig. 3, and $2J_0$ is the exchange coupling at the position $\min_s[r_{s(ij)}] = R_0$. The parameters $(\gamma, R_0, J_0) = (43\ \text{nm}^{-1}, 0.32\ \text{nm}, 20\ \text{K})$ successfully reproduce the distortion of the HC phase of the O_2 lattice [13,19], confirming the validity of the model. As listed on Table I, the model that includes only electric interactions results in an isosceles triangular lattice as mentioned before. On the other hand, the result additionally including the exchange interaction produced the lattice distortion comparable to the one observed experimentally. Thus, we concluded that the antiferromagnetic

FIG. 3. Nearest-neighbor distances between nonbonding oxygen atoms with respect to various configurations.

TABLE I. MC calculations for LC phase of the O_2 lattice.

$\mathcal{H}$	AB (nm)	AC (nm)	$\angle BAC$ (deg.)
Our experiment	0.421	0.435	42.8
Calculation without $\mathcal{H}_{Ex}$	0.425	0.425	47.9
Calculation with $\mathcal{H}_{Ex}$	0.414	0.434	47.3

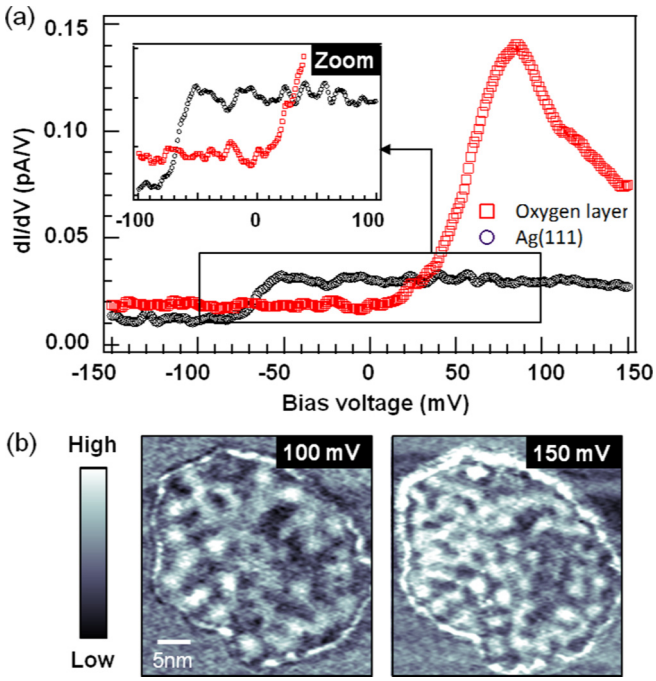

FIG. 4. (a) dI/dV spectra taken on O_2-covered and bare Ag(111) surfaces without annealing. (b) dI/dV mappings acquired on the O_2 island [(a) bias modulation: $V_{mod} = 7$ mV; (b) left image: $V_s = 100$ mV, $V_{mod} = 10$ mV; right image: $V_s = 150$ mV, $V_{mod} = 10$ mV].

ordering of the O_2 spins played a crucial role in the distortion of the O_2 lattice on Ag(111).

In order to verify the preservation of the intrinsic $S = 1$ spin of O_2 on the Ag(111) surface, we carefully checked the dI/dV spectra taken on the O_2 island and bare Ag(111) surface, as displayed in Fig. 4(a). The spectrum on the Ag(111) surface showed the onset of the Shockley surface state at around -68 mV [21–23], and its energy level shift by $\sim$100 mV due to the presence of the O_2 layer has been observed like many other physisorbed monolayers on noble-metal (111) surfaces [17,24]. This is also supported by the observation of bias-dependent standing wave patterns on the O_2 island shown in Fig. 4(b) (see the Supplemental Material for details of the dispersions [13]). Note that no specific evidence of the Kondo resonance was detected around the Fermi level at 4.7 K in spite of the presence of a localized spin of the O_2 molecules in the metallic host [see the inset of Fig. 4(a)]. This is quite different from the case of the 2D O_2 lattice physisorbed on the Ag(110) surface, which exhibited a clear Kondo resonance at 18 K [25].

In the framework of the Anderson model [26], which is simplified as a single magnetic impurity in a host metal, important factors for the resonance are the electron transfer between the impurity and the metallic states (V), and the density of states at the Fermi level (ρ_0). TDS measurements showed that the adsorption energy of O_2/Ag(111) was lower than that of O_2/Ag(110) estimated from the desorption peak [O_2/Ag(111): 35 K [11], O_2/Ag(110): 59 K [27]]. This indicates that V between the O_2 spin and Ag(111) metallic states is less than that between the O_2 spin and Ag(110) states. ρ_0 in O_2/Ag(111) can be reduced because of the lack of surface electrons on the O_2 layer due to the modification of the surface state mentioned before [28,29]. In addition, O_2 molecules form a 2D lattice, unlike the Anderson single-impurity model. Hence, the intermolecular antiferromagnetic interaction can also contribute to hinder the Kondo resonance in this system [30,31]. Thus, we concluded that the O_2 spins are little influenced by the itinerant electrons of the substrate, and would be expected to form an $S = 1$ quantum spin system.

In conclusion, we report on real-space observation of surface phase of O_2 physisorbed on an Ag(111) surface with low-temperature STM/STS. The desorption of almost all O_2 from the Ag(111) surface after the 40 K annealing confirmed the physisorbed state of O_2. The observed molecular lattice of the O_2 island revealed its scalene triangular lattice. We ascribe the lattice distortion from the isosceles triangular lattice to the antiferromagnetic ordering of the O_2 spins and the softness of the O_2 lattice. We confirmed this scenario by reproducing the lattice distortion quantitatively through MC calculations. In dI/dV spectra, no evidence of the Kondo resonance down to 4.7 K was observed. These results imply that our system is an example of a 2D $S = 1$ antiferromagnetic quantum spin system and the potential for a brand-new approach constructing low-dimensional quantum spin systems in a bottom-up fashion.

We thank K. Fukutani, T. Kawae, E. Kazuma, H. Kim, and E. Minamitani for fruitful discussions and valuable comments. This work was partially supported by JSPS KAKENHI Grants No. 25707025, No. 26120508, and No. 26110507 (Grants-in-Aid for Scientific Research on Innovative Areas "Molecular Architectonics: Orchestration of Single Molecules for Novel Functions"), and also by Foundation of Advanced Technology Institute, Japan.

[1] Y. Freiman and H. Jodl, Phys. Rep. **401**, 1 (2004).
[2] G. C. DeFotis, Phys. Rev. B **23**, 4714 (1981).
[3] L. Balents, Nature (London) **464**, 199 (2010).
[4] F. Haldane, Phys. Lett. A **93**, 464 (1983).
[5] Y. Murakami, J. Phys. Chem. Solids **59**, 467 (1998).
[6] T. Shibata, Y. Murakami, T. Watanuki, and H. Suematsu, Surf. Sci. **405**, 153 (1998).
[7] R. Kitaura, S. Kitagawa, Y. Kubota, T. C. Kobayashi, K. Kindo, Y. Mita, A. Matsuo, M. Kobayashi, H.-C. Chang, T. C. Ozawa, M. Suzuki, M. Sakata, and M. Takata, Science **298**, 2358 (2002).
[8] A. Hori, T. C. Kobayashi, Y. Kubota, A. Matsuo, K. Kindo, J. Kim, K. Kato, M. Takata, H. Sakamoto, R. Matsuda, and S. Kitagawa, J. Phys. Soc. Jpn. **82**, 084703 (2013).
[9] M. Hagiwara, M. Ikeda, T. Kida, K. Matsuda, S. Tadera, H. Kyakuno, K. Yanagi, Y. Maniwa, and K. Okunishi, J. Phys. Soc. Jpn. **83**, 113706 (2014).
[10] A. A. Khajetoorians, J. Wiebe, B. Chilian, S. Lounis, S. Blügel, and R. Wiesendanger, Nat. Phys. **8**, 497 (2012).
[11] Y. Kazama, M. Matsumoto, T. Sugimoto, T. Okano, and K. Fukutani, Phys. Rev. B **84**, 064128 (2011).

[12] K. Niki, S. Ogura, M. Matsumoto, T. Okano, and K. Fukutani, Phys. Rev. B **79**, 085408 (2009).

[13] See Supplemental Material at http://link.aps.org/supplemental/10.1103/PhysRevB.93.081408 for a detailed analysis of the thickness for the oxygen layer, the tip effect, the dispersion relation of the oxygen layer, and Monte Carlo calculations.

[14] M. Kulawik, H.-P. Rust, N. Nilius, M. Heyde, and H.-J. Freund, Phys. Rev. B **71**, 153405 (2005).

[15] M. F. Toney and S. C. Fain, Phys. Rev. B **36**, 1248 (1987).

[16] R. D. Etters, R. P. Pan, and V. Chandrasekharan, Phys. Rev. Lett. **45**, 645 (1980).

[17] L. Bruch, M. Cole, and E. Zaremba, *Physical Adsorption: Forces and Phenomena*, Dover Books on Physics (Dover, New York, 2007).

[18] Y. Murakami, I. Makundi, T. Shibata, H. Suematsu, M. Arai, H. Yoshizawa, H. Ikeda, and N. Watanabe, Phys. B (Amsterdam, Neth.) **213-214**, 233 (1995).

[19] R. D. Etters and O. B. M. Hardouin Duparc, Phys. Rev. B **32**, 7600 (1985).

[20] A. J. R. da Silva and L. M. Falicov, Phys. Rev. B **52**, 2325 (1995).

[21] L. Bürgi, O. Jeandupeux, A. Hirstein, H. Brune, and K. Kern, Phys. Rev. Lett. **81**, 5370 (1998).

[22] F. Reinert, G. Nicolay, S. Schmidt, D. Ehm, and S. Hüfner, Phys. Rev. B **63**, 115415 (2001).

[23] O. Jeandupeux, L. Bürgi, A. Hirstein, H. Brune, and K. Kern, Phys. Rev. B **59**, 15926 (1999).

[24] J. Y. Park, U. D. Ham, S.-J. Kahng, Y. Kuk, K. Miyake, K. Hata, and H. Shigekawa, Phys. Rev. B **62**, R16341(R) (2000).

[25] Y. Jiang, Y. N. Zhang, J. X. Cao, R. Q. Wu, and W. Ho, Science **333**, 324 (2011).

[26] P. W. Anderson, Science **235**, 1196 (1987).

[27] R. Franchy, F. Bartolucci, F. B. de Mongeot, F. Cemic, M. Rocca, U. Valbusa, L. Vattuone, S. Lacombe, K. Jacobi, K. B. K. Tang, R. E. Palmer, J. Villette, D. Teillet-Billy, and J. P. Gauyacq, J. Phys.: Condens. Matter **12**, R53 (2000).

[28] H. Manoharan, C. Lutz, and D. Eigler, Nature (London) **403**, 512 (2000).

[29] J. Henzl and K. Morgenstern, Phys. Rev. Lett. **98**, 266601 (2007).

[30] H. Prüser, P. E. Dargel, M. Bouhassoune, R. G. Ulbrich, T. Pruschke, S. Lounis, and M. Wenderoth, Nat. Commun. **5**, 5417 (2014).

[31] E. Minamitani, H. Nakanishi, W. Agerico Diño, and H. Kasai, Solid State Commun. **149**, 1241 (2009).